

# Globular vs. Open Cluster HR Diagrams

*Physics Department, University of California, Santa Barbara, CA 93106*

(Dated: submitted June 14, 2023)

There are two main types of stellar clusters: globular and open. We take observations of one of each of these clusters to compare the resulting Hertzsprung-Russell (HR) diagrams. We use the Las Cumbres Observatory (LCO) observation request program to observe M6 and M13. These are open and globular clusters respectively. We requested 4 SDSS filters:  $u'$ ,  $g'$ ,  $r'$ , and  $i'$ , with 10 exposures for 10 seconds for each filter. The resulting FITS files were analyzed to extract data from them. We can use this data to determine that these clusters differ greatly in age and brightness.

## I. INTRODUCTION

HR diagrams are scatter plots of a star's apparent magnitude versus its color index which represents temperature [1]. These diagrams are extremely important in classifying stars, determining ages of clusters, determining the life cycle of a given star, and much more. They are created using observations of a cluster of stars or galaxy and determining the flux value of each star. You can then use color indices to determine their temperatures. A color index is the difference in magnitude from one filter to another.

The clusters that we are looking at are M6 and M13. M6 is an open cluster commonly referred to as the Butterfly Cluster. It is located in the constellation Scorpius at approximately  $1.6 \times 10^3$  light years away with around 300 stars. It was first observed by Giovanni Battista Hodierna in 1654 and was named by Robert Burnham because it was said that the outline looks like opening butterfly wings [2]. The brightest star is BM Scorpi (a K-type orange giant star) of variable magnitude from 5.5 to 7. M13 is a globular cluster commonly referred to as the Hercules Globular Cluster due to its location in the constellation of Hercules. It is about  $2.22 \times 10^4$  light years away and has about 300,000 stars. It was first discovered in 1714 by Edmond Halley [3]. The brightest star the variable star V11 (a red giant) of magnitude 11.95.

## II. SIGNIFICANCE

HR diagrams were first used in 1911 when Ejnar Hertzsprung plotted stars' apparent magnitudes versus their colors. Henry Norris Russell then independently did the same thing except with apparent magnitudes and spectral classes [4]. HR diagrams hold information about common types of stars. Stars and objects with more complex properties cannot be modeled with HR diagrams, but they are extremely important for understanding properties of common stars.

The most common forms of HR diagrams are apparent

magnitude versus either temperature or spectral class. Many will also include both, along with luminosity along the four axes. These are important properties of stars conveniently represented in one place. This also describes the age and type of star. The main sequence is a diagonal path from the upper left to the lower right which represents the majority of stars, around 90%. Other types of stars can be classified by these diagrams too like white dwarfs, supergiants, giants, etc.

The age of stars can also be determined from HR diagrams. Stars that began on the main sequence will move off to turn into different types of stars as they age. They then move into another category of star which can have the age determined by the properties given in the diagram. This can also be used for star clusters. The turn off point can help determine the age of the stars in the cluster as it is the amount of stars that have moved off of the main sequence. This gives an immense amount of information about a given cluster and allows them to be compared to other clusters. As we will see, they create very different looking HR diagrams.

## III. APPROACH

### A. Data Collection

We received data from the Las Cumbres Observatory by putting in a request for observation. We requested the use of the filters SDSS  $u'$ , SDSS  $g'$ , SDSS  $r'$ , and SDSS  $i'$  for both clusters [6]. The details of the filters are described in the graphic from LCO in Figure 1. We requested 10 second exposures with 10 images taken for each filter. We also had to make sure that the clusters were visible for at least one of the available telescopes during this time of year. To determine this, we use LCO's visibility tool [5]. The daily visibility of M6 and M13 are shown in Figures 2 and 3 respectively.

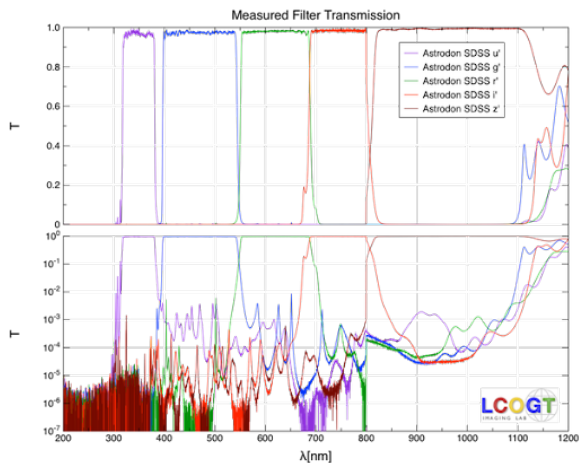


FIG. 1: The wavelengths and transmissions for each SDSS filter. We notice that the visible light spans filters  $g'$  and  $r'$ .

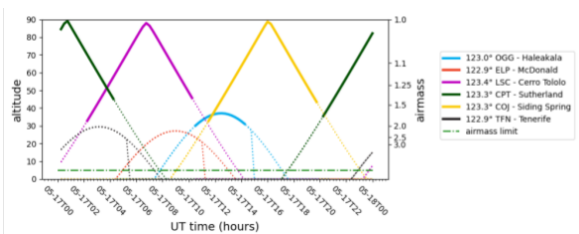


FIG. 2: This is the visibility of the cluster on May 15th. This is representative of the visibility of M6 during the season that the observation took place. The best observation time would be at the peak altitude as there is the least amount of airmass obstruction. The images were indeed taken around 7:20 UTC on the Cerro Tololo which is around the peak altitude at that location.

## B. Images

### 1. Extraction

Once the images are received in the form of FITS files, there needs to be some post processing before we can use them. We need to stack each of the 10 second images together in order to get better data about the cluster. To do this, we use a program called Astroart. In this program, you can align and stack images into essentially a 100 second exposure with our 10 images for each filter. We can do this with every filter. Each filter for M6 is shown in Figure 4. We can then combine all of the filters with the Trichromy function in Astroart. We used SDSS  $g'$ ,  $r'$ , and  $i'$  to create our combined images as these represent the visible wavelengths (Figure 5). We can then do the same with M13 as seen in Figures 6 and 7. We did not use the SDSS  $u'$  filter because as it turns out, it

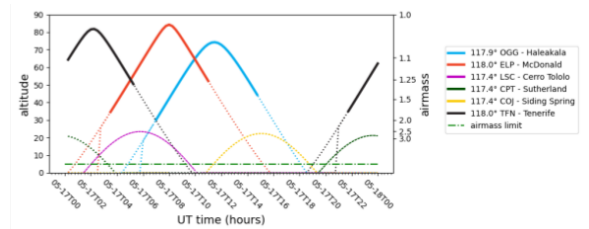


FIG. 3: This is the visibility of M13 again on May 15th.

These images were taken by the Tenerife telescope around 22:60 UTC. This is not as close to the peak, but it is also not too close to where the airmass becomes a problem.

did not give us any significant data.

Once we have these stacks of each individual filter, we can then begin to extract sources. We use a library called Source Extraction and Photometry (SEP) to detect the sources from the image [7]. However, in order for SEP to interpret information from the FITS files, we have to swap the byte order on the FITS files. Once we have done this we can use the `sep.Background()` and the `sep.extract()` functions. We then input the image with the background subtracted off of it and set the threshold of detection to 3 times the root mean squared of the background with the center point spread function set to 5 pixels. The aim of this is to pick out sources, not noise. This function then outputs a considerable amount of information about the file that was inputted, including coordinates of the source. We then plotted the sources found (indicated by a red circle) over our images to ensure that it is working properly. The results of this are shown in Figure 8. However, there is a problem with M13. The center of the cluster has so many stars in the same place that SEP cannot accurately distinguish between stars. We then have to mask this area so it does not skew the data with extremely large flux values. To do this, we cut out that center area so those sources are not including as shown in Figure 9.

We can then use these outputs to determine the magnitude of each source in each filter with the function:

$$m = -2.5 \log_{10}(N_{\text{aperture sum}}) \quad (1)$$

However, SEP can pick out different sources in the two filters. We then have to cross match each of the extraction positions to make sure that we are only using the same sources across both filters.

### 2. Color Index

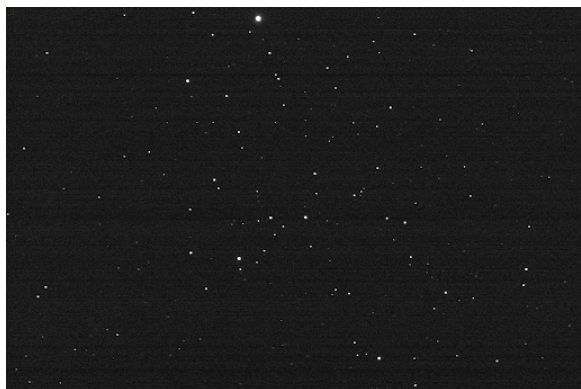
Once we have this for both the  $g$  filter and the  $r$  filter, we can then determine the color index. We used the  $g$



(a)



(b)



(c)

FIG. 4: Filter images for M6: (a) Stacked images of SDSS  $g'$ ; (b) Stacked images of SDSS  $r'$ ; and, (c) Stacked images of SDSS  $i'$

and  $r$  filter because these are just different naming conventions for the usual color indices  $B$  and  $V$ . The most common color index used in HR diagrams is  $B-V$ . We subtract these indices because this is a difference in magnitude, which gives us the color of the object. We can



FIG. 5: Trichromy of M6. This creates a color image of the cluster as we observed it.

then write this using equation 1 as:

$$B - V = -2.5 \log_{10} \left[ \frac{\int d\lambda S_B(\lambda) F_\lambda}{\int d\lambda S_V(\lambda) F_\lambda} \right] + C_{B-V} \quad (2)$$

The integrals here represent the sensitivity function of the filter multiplied with the spectral energy distribution of the source. The  $C_{B-V}$  is a magnitude calibration that will be described later. For our purposes we can use the SEP functions `CircularAperture` and `aperture_photometry`. This is a benefit of using source extractor as it has built in functions to do these calculations.

## IV. RESULTS

### A. Initial HR Diagrams

Now that we have the magnitudes and the color indices, we can plot the apparent magnitudes versus the color index to get our HR diagram. The initial HR diagrams can be seen in Figure 10. There are many outliers in each of these diagrams. We do not want to include these in our data as they are most likely not stars actually in the cluster. These could be stars that are in between the Earth and the cluster or they could even be noise values picked out by SEP. In order to eliminate these outliers, we need to use a python function called `SigmaClip`. We can use this to define the mean and standard deviation of the sources. With this, we can subtract off a certain number of standard deviations from the mean. In doing this, we can eliminate our outliers from the data set.

For M13, the outliers do not seem too extreme. We can take 3 sigma from the mean and get a good representation of our data. However, for M6 it is more complicated. M6 only has around 300 stars in the cluster. SEP extracted



(a)



(b)



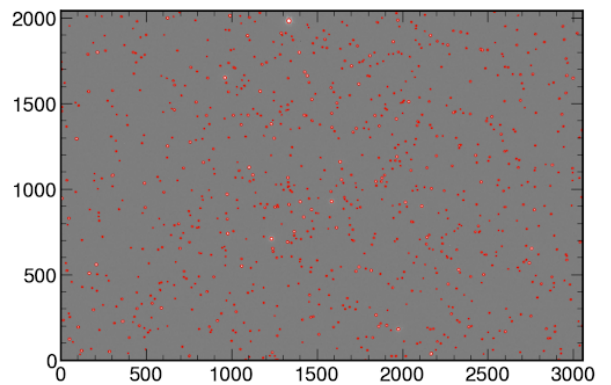
(c)

FIG. 6: Filter images for M13: (a) Stacked images of SDSS  $g'$ ; (b) Stacked images of SDSS  $r'$ ; and, (c) Stacked images of SDSS  $i'$

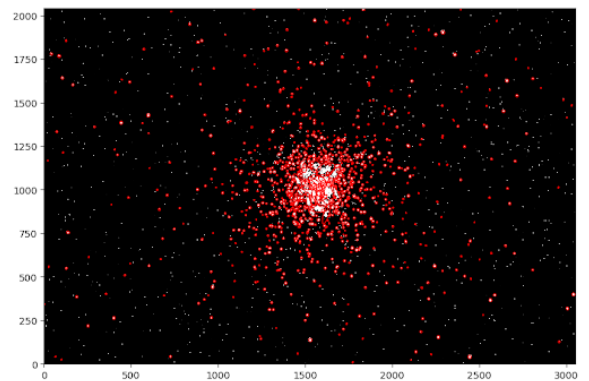
675 sources, so we know that we need to take out a decent amount of those found sources. We can also see this visually in the diagram that we have sources that are very far off from the cluster. In using a one sigma range, we find the best representation of the data. For most data sets this would be an extreme amount of data to discount. However we see that there are many stars concentrated around the mean and we know that the initial data set



FIG. 7: Trichromy of M13. Notice that this image is a lot less blue than M6. This makes sense as M6 has many young blue stars and M13 has mostly older orange/red stars.



(a)



(b)

FIG. 8: The result of SEP: (a) for M6. The grayscale is a lot lighter here because the sources in M6 are very bright, making this the best way of viewing it.; (b) for M13. We can see that in the center it has picked out more than one source in the center of the images where there many stars in the same space.



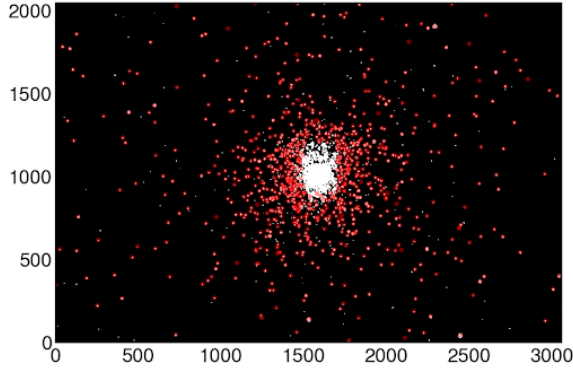


FIG. 9: We have taken out all of the extraction points that picked out more than one source. We can now see that every source is clearly defined.

had too many sources.

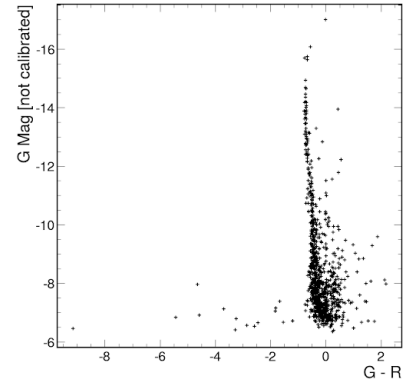
With these initial HR diagrams we can see that we are seeing instrumental magnitudes. Negative magnitudes do not make sense to represent this data. Negative magnitudes are generally extremely bright objects in our sky like the moon or the sun. We know that we are going to have to make an adjustment to get the true apparent magnitudes.

### B. Magnitude Calibration

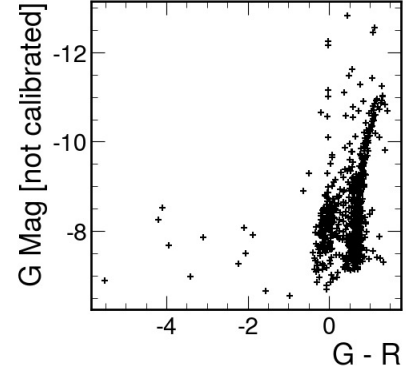
To represent the correct apparent magnitudes, we need to use reference stars. Reference stars are stars that we choose within the field to use a star atlas and determine the apparent magnitude. We again used Astroart to achieve this. Astroart has a Star Atlas function in which you can match your field to the atlas and choose the stars you want to find the magnitude of. We chose five reference stars for each cluster. Our choices are shown in Table I.

Once we have all of the reference stars, we need to find them in our data set. To do this, we use the functions within the packages `astropy.coordinates` and `astropy.wcs`. In these packages we can use the `Angle` function which takes an input of strings. We can use this on our right ascensions and declinations to find the angles associated. We can then use the `SkyCoord` and `skycoord_to_pixel` functions to extract the pixel values of these locations [8]. We can again make sure that this worked properly by plotting the pixel values over our images as shown in Figure 11.

Now that we have these locations and magnitudes in terms of pixels in our images, we can create a linear fit to find the  $C_{B-V}$  value. To do this, we plot the apparent magnitude determined by the star atlas, versus



(a)



(b)

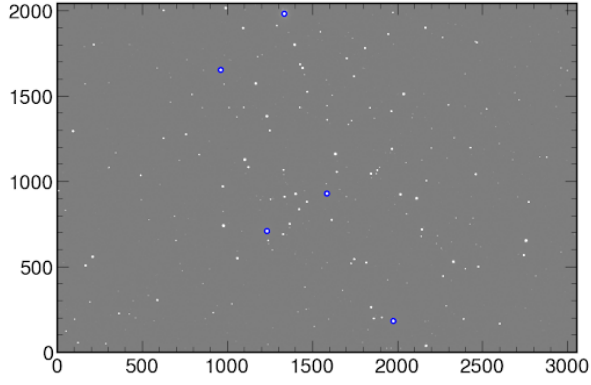
FIG. 10: Initial HR Diagrams with raw data: (a) for M6. We can see many outliers from our main cluster.

We can also see that the magnitude seems to span many different brightnesses; (b) for M13. We can also see many outliers here. However, there is not as wide a range of magnitudes.

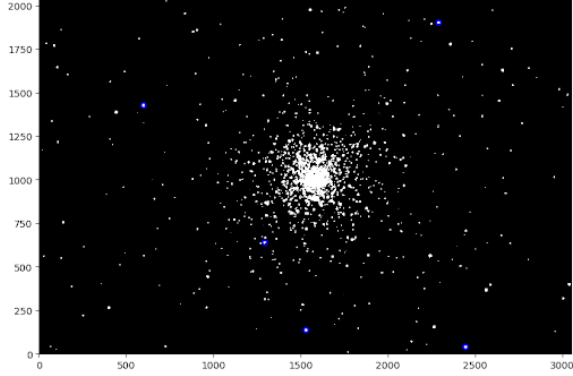
Cluster	Reference Stars		
	Right Ascension	Declination	Magnitude
M6	17:39:37.6	-32:19:13	7.12
	17:40:01.0	-32:12:04	6.70
	17:40:11.1	-32:15:24	7.21
	17:40:43.4	-32:09:21	7.21
	17:40:58.5	-32:12:52	5.24
M13	16:40:54.9	+36:19:22	10.17
	16:40:59.7	+36:28:04	10.60
	16:41:23.5	+36:30:17	11.52
	16:42:01.1	+36:36:51	11.66
	16:42:22.9	+36:20:43	10.34

TABLE I: Positions and magnitudes of chosen reference stars for each cluster.

the instrumental magnitude found from SEP. Once we have done this, we can fit a line to the data and use the



(a)



(b)

FIG. 11: (a) Pixel values for M6 reference stars. They do indeed match the locations of the chosen reference stars.; (b) Pixel values for M6 reference stars. These also correctly matched the locations of the chosen reference stars.

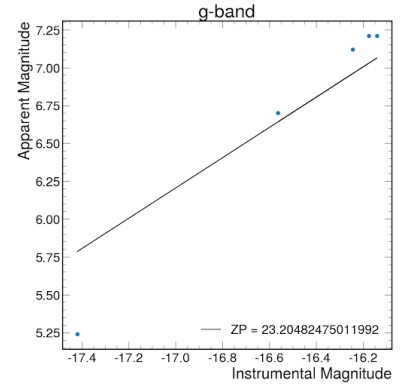
difference in the intercept values from each filter as our correction. Plots are shown in Figure 12.

Now that we have these values, we can add them to our apparent magnitudes to get the calibrated HR diagrams. The final diagrams are shown in Figure 13.

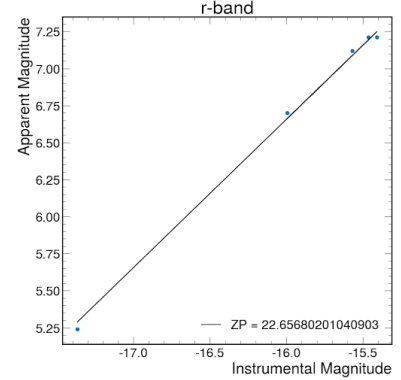
### C. Error Analysis

We have 2 main sources of error: counting error from brightness and error from the linear fit. The error in brightness then has to be propagated to a magnitude as that is the final value that we are reporting. The formula for error propagation is:

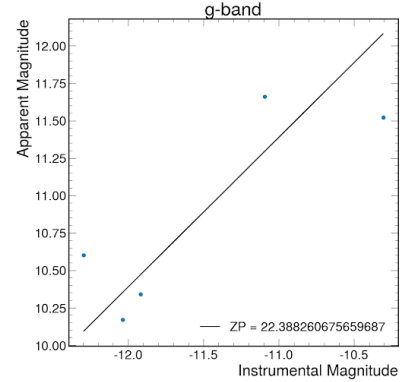
$$\sigma_f = \sqrt{\left(\frac{\partial f}{\partial x}\right)^2 \sigma_x^2} \quad (3)$$



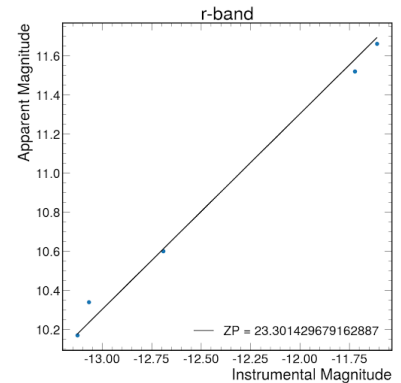
(a)



(b)

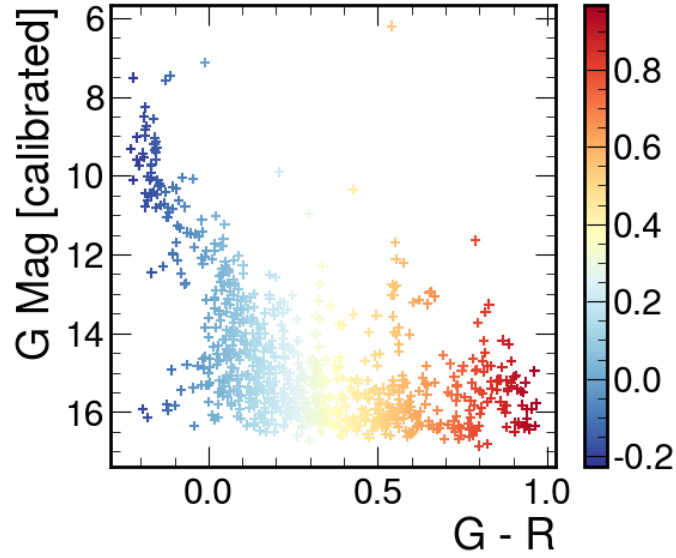


(c)

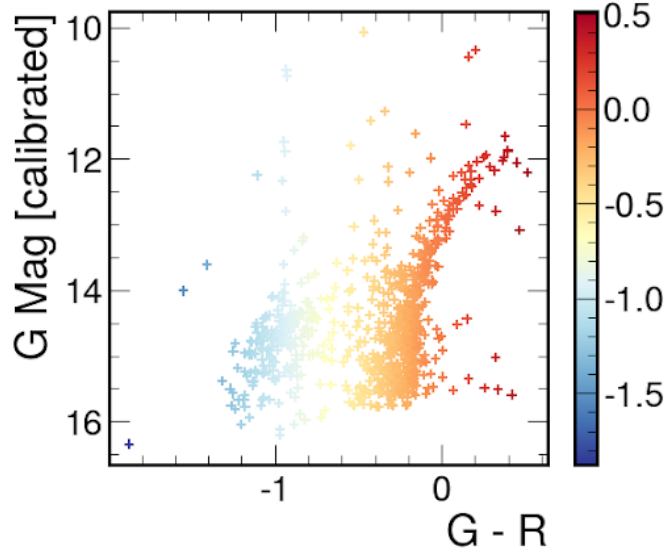


(d)

FIG. 12: Zero correction values given as ZP in the bottom right corner for each filter. We notice that both g-band filters do not seem to have very good fits while the r-bands seem to fit pretty well. We do not really know why this is. (a) M6 g-band linear fit.; (b) M6 r-band linear fit.; (c) M13 g-band linear fit.; (d) M13 r-band linear fit.



(a)



(b)

FIG. 13: (a) Calibrated M6 HR diagram with a color map based on the color index values. While this might not be the exact colors at each point, it provides a good visualization.; (b) Calibrated M13 HR diagram with a color map based on the color index values.

Using equation 3 we can see that the error in magnitude is

$$\sigma_M = \sqrt{\left(\frac{-2.5}{B \times \ln(10)}\right)^2 \sigma_B^2} \quad (4)$$

$$\sigma_M = \frac{2.5}{S/N \times \ln(10)} \quad (5)$$

So now we need to be able to calculate the signal to noise ratio (SNR). To do this we need some descriptive values about sources of noise. One of those is quantum

efficiency. Quantum efficiency is the ability of the telescope to convert photons to electrons [9]. The quantum efficiency of the CCD image sensor used is 65% for red wavelengths and decreases for smaller wavelengths. Dark current is redundant excitations of the camera, often due to temperature. Background noise is from light pollution captured by the telescope. Readout noise involves left-over electrons from previous images that are recorded in following CCD readouts. All of these factors contribute to the SNR through a series of calculations [10]. The first

Readout Noise	14.5 $e^-$
Dark Current	0.03 @ -100 C (estimated) $e^-/\text{pix-s}$
Background estimation	$N_B = \sqrt{\pi r_{pho}^2 \mu_{bkg}}$

TABLE II: Values for SNR equation

	M13	M6
SNR-g'	76.152 dB	87.440 dB
SNR-r'	81.078 dB	82.402 dB
$\sigma_M$	0.00976	0.00904

TABLE III: SNR values for each filter and cluster along with the error it causes in the magnitude.

of which involves the quantum efficiency:

$$S = F\tau A\epsilon Q_e \quad (6)$$

This represents the flux readout, integration time, area of the telescope, telescope transfer efficiency and quantum efficiency. Luckily, we are able to use SEP for the first part and all we need to do is multiply by the quantum efficiency. We know that the SNR is signal over total noise. The total noise will be

$$N_T = \sqrt{N_S^2 + N_R^2 + N_{DC}^2 + N_B^2} \quad (7)$$

This makes the total SNR equal to

$$\frac{S}{N} = \frac{F\tau A\epsilon Q_e}{\sqrt{N_R^2 + \tau(FA\epsilon + i_{DC} + F_B A\epsilon Q_e \Omega)}} \quad (8)$$

With  $\Omega$  being the solid angle of the pixel and the values listed in II.

The SNR and subsequently the error in magnitude, using  $\sqrt{\sigma_g^2 + \sigma_r^2}$  for total propagated SNR, using equations 5 and 8 are listed in III

The other source of error is from the calibration best fit line. We calculate the error from this with root mean square deviation. The formula for this is

$$RMSD = \sqrt{\frac{\sum_{i=1}^N (x_i - \hat{x}_i)^2}{N}} \quad (9)$$

Which gives the error values in table IV. Propagating these through, we just add the two values making the error for data points in M13:  $\sigma_M = \pm 0.40276$  and in M6:  $\sigma_M = \pm 0.28704$ .

	M13	M6
RMSD g'	0.389	0.276
RMSD r'	0.0563	0.0365
Total	0.393	0.278

TABLE IV: Error in linear fits for each filter and cluster along with the total error from them.

## V. DISCUSSION

### A. M6

When comparing our diagram to the photometric study, we can see the general shape and similar magnitudes found [11]. We can directly compare these diagrams as G-R is just a naming convention of the filters that represent B-V (Figure 14). The magnitudes are very low values in both diagrams indicating very bright stars. We also see the general pattern of the main sequence in both diagrams. This indicates that this cluster should represent a relatively new cluster. There is no distinct turn off point as seen meaning that most of the stars are still in the main sequence.

As mentioned in the sigma clip section, we did not have the time or resources to do an analysis of motion or surface density as a function of distance to the center, so we had to use conventions of previous work [11]. There also appears to be more stars even in our sigma clipped diagram than the reference diagram. This could also be due to the fact that we cannot determine which stars are actually in the cluster versus stars in between the telescope and cluster or noise that source extractor picked out as a source. This could cause an excess of stars along with the fact that the field was larger than just the cluster so it included other stars. Other studies have determined the age of this cluster to be around  $1.0 \times 10^8$  yr which fits the result of a young cluster from the HR diagram.

### B. M13

Comparing our final HR diagram with the reference from Gaia Data, we can say that we similar shape and scale (Figure 15) [12]. We see quite a turn off from what we would know as the main sequence and some different groups in this diagram. The major groups we have here are red giants and supergiants (right side), blue giants (upper left) and horizontal branch stars (lower left). There are also smaller groups of asymptotic-giant-branch (far right) and "blue straggler" (lower more neutral blues and greys) stars.



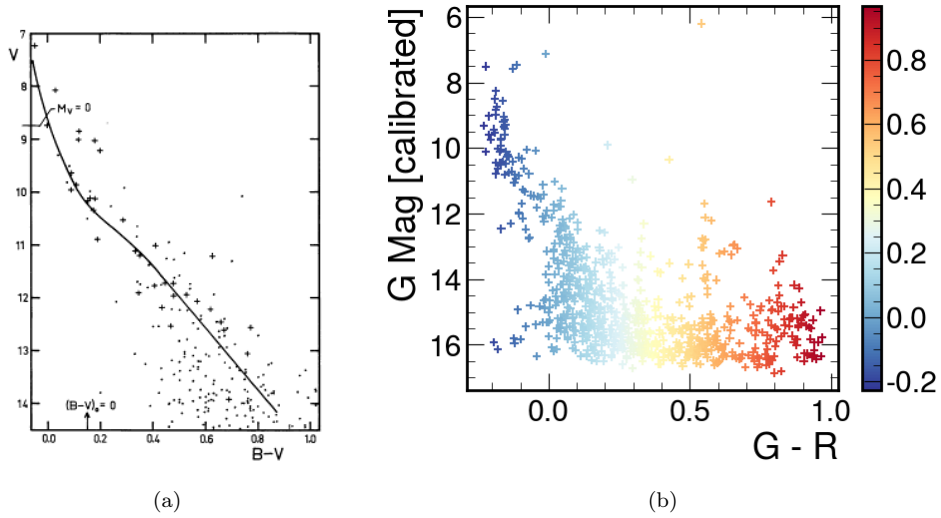


FIG. 14: (a) This is the HR diagram of a previous study of M6. This has been filtered based on surface density as a function of distance to the center to make sure that it just includes the stars from the cluster. They did also use Kodak filters and we have much better technology now.; (b) We can see the similar shape of the main sequence that is in the reference HR diagram. You can also see the brightest star at the top around magnitude 6 in the orange color range. We see no turn off point as this is a young cluster and still has most of its stars still in the main sequence.

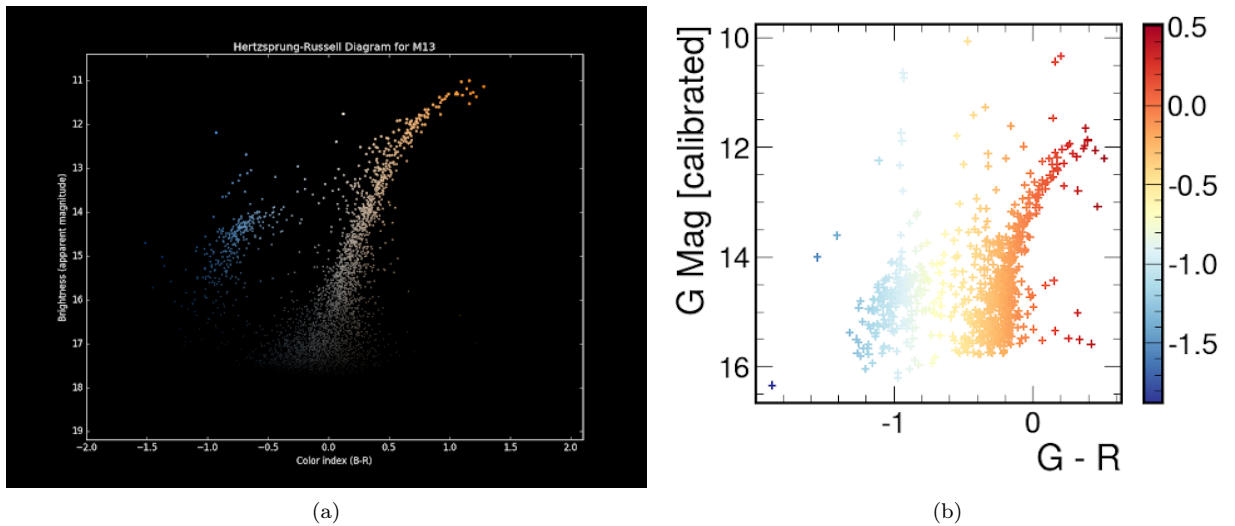


FIG. 15: (a) This is the HR diagram of an astronomy picture of the day from 2019. The specific filters used were not stated, but it is assumed they are much more modern than the study for M6. It is difficult to see but we can see the blue group on the left and the right red group.; (b) We can see the similar shape of the groups in our diagram to the reference diagram. The range of magnitudes is also very similar. This is thus very promising that our HR diagram is close to accurate. It is hard to pick out the brightest star as we may still have some extraneous stars in the diagram.

### C. Comparison

We can clearly see the difference between the two clusters. From our data and diagrams we can see that globular clusters are older, meaning they are also dimmer, and actually contain some of the oldest stars in the galaxy.

Open clusters have much less stars that are young and bright. They are the recent formations of stars from gas clouds [14]. Our HR diagrams are extremely helpful in noticing the differences and classifications of the stars in each cluster. The color mapping especially helps for visualization of the color indices and the colors they rep-

resent.

### D. Improvements

One thing to improve this process is taking data over longer periods of time to see the motion of stars. This could help identify which stars are actually in the cluster. There are also some stars in M13 that are too dim to detect. A larger telescope or even an improved detection method (possibly machine learning) would possibly help detect this star and more accurately represent the cluster. There were also issues with the accuracy of the zero

point shift in the g-filter. This could be due to many reasons, but the most likely being that we only acquired one magnitude from star atlas that we used for both filters. The filters seemingly do not have a linear relationship causing more error with one filter over another.

### VI. ACKNOWLEDGEMENTS

I would like to thank my partners for this project, Audrey O'Malley and Linda Jin. I would also like to thank Dr. Lubin, Sam Whitebook, and Jeonghwa Kim. I would also like to thank LCO for the data and resources.

- 
- [1] Las Cumbres Observatory. *Magnitude and Color*. Space Book (8). <https://lco.global/spacebook/distance/magnitude-and-color/>
  - [2] Messier Objects admin (2015). *Messier 6: Butterfly Cluster*. Messier Objects (6). <https://www.messier-objects.com/messier-6-butterfly-cluster/>
  - [3] Messier Objects admin (2015). *Messier 13: Hercules Globular Cluster*. Messier Objects (13). <https://www.messier-objects.com/messier-13-hercules-globular-cluster/>
  - [4] Las Cumbres Observatory. *H-R Diagram*. Space Book (3). <https://lco.global/spacebook/stars/h-r-diagram/>
  - [5] Las Cumbres Observatory. *Visibility Tool*. <https://lco.global/observatory/tools/visibility/>
  - [6] Las Cumbres Observatory. *Filters*. <https://lco.global/observatory/instruments/filters/>
  - [7] Kyle Barbary and contributors (2016). *Reference/API*. <https://sep.readthedocs.io/en/v1.0.x/reference.html>
  - [8] The Astropy Developers (2023). *Astronomical Coordinate Systems (astropy.coordinates)*. <https://docs.astropy.org/en/stable/coordinates/index.html>
  - [9] Teledyne Photometrics (2023). *Introduction To Quantum Efficiency*. Imaging Topics. <https://www.photometrics.com/learn/imaging-topics/quantum-efficiency>
  - [10] Lubin, P. (2016). The Search for Directed Intelligence. *REACH*, 26-27.
  - [11] Vleeming, G. (1974). A photometric study of the open cluster M6 (NGC 6405). *Astronomy and Astrophysics Supplement Series* (16), 331-342.
  - [12] Vanderbei, B (2019). *Hertzsprung-Russell Diagram for M13*. Hertzsprung-Russell Diagrams for Globular and Open Clusters, <https://vanderbei.princeton.edu/images/NJP/HRdiag.html>
  - [13] McClure, B. & Machholz, D. (2022). *Meet M13, the Great Cluster in Hercules*. Clusters Nebulae Galaxies. <https://earthsky.org/clusters-nebulae-galaxies/m13-finest-globular-cluster-in-northern-skies/>
  - [14] Astronomy Staff. (2019). *What is the difference between a globular star cluster and an open star cluster?*. <https://www.astronomy.com/science/what-is-the-difference-between-a-globular-star-cluster-and-an-open-star-cluster/>

## Appendix A: Code

All code that was written for this is contained in <https://github.com/Klinjin/134L/tree/main>

## Appendix B: Picture



Helix Nebula. Because I like it.